

Data Efficient Contrastive Learning in Histopathology using Active Sampling

Tahsin Reasat¹ and David S. Smith^{1,2}

1. Vanderbilt University, Department of Electrical and Computer Engineering; 2. Vanderbilt University Medical Center, Department of Radiology and Radiological Sciences

Abstract—Deep Learning based diagnostics systems can provide accurate and robust quantitative analysis in digital pathology. These algorithms require large amounts of annotated training data which is impractical in pathology due to the high resolution of histopathological images. Hence, self-supervised methods have been proposed to learn features using ad-hoc pretext tasks. The self-supervised training process is time consuming and often leads to subpar feature representation due to a lack of constrain on the learnt feature space, particularly prominent under data imbalance. In this work, we propose to actively sample the training set using a handful of labels and a small proxy network, decreasing sample requirement by 93% and training time by 62%.

Index Terms—Digital Pathology, Deep Learning, Active Learning, Contrastive Learning, Self Supervised Learning

I. INTRODUCTION

The recent renaissance of self-supervised learning (SSL) began with artificially designed pretext tasks, such as relative patch prediction [1], solving jigsaw puzzles [2], colorization [3] and rotation prediction [4]. Recently, contrastive learning (CL) has emerged as a simple yet promising tool in SSL [5]. It has been successfully applied to cancer detection, segmentation in histopathology images [6]. In practice, the CL model is trained using a large unlabeled data pool, and the extracted features from this large model are used to train a smaller linear model, and its prediction is evaluated on a test set to measure its performance (*linear evaluation*) [5].

The training phase is slow and learned latent space is unconstrained, which could be suboptimal for histopathological datasets. Histopatholog-

ical datasets often have a lot of confounding image sections consisting of background and debris alongside normal tissue area. Additionally, the tissue of interest is normally the cancerous tumor area which is often a minority class. As a result the model either takes too many iterations to learn the minority class examples or, even worse, ignores the minority class and uses all its capacity to learn the non-tumor cells. We propose to solve these inefficiencies by borrowing techniques from *active learning*.

Active learning [7], [8] allows humans to interactively improve algorithms. The algorithm is trained iteratively using an algorithmically sampled data subset (*active sampling*) which is labeled by an oracle (e.g., human annotator). In each iteration, new informative subset of samples is chosen to further train and improve model predictions Fig. 1. Multiple datasets have been produced by user refined inputs such as automatic teller machine, self-driving cars, automatic content tagging in online platforms [9]. Active learning has proven useful in annotating data when specialist input is required, e.g. medical images [10].

To decrease data redundancy, we propose to train the network iteratively using batches of unlabeled data. The first batch is randomly selected and after training the model on each batch, we select the next batch of data from the unlabeled pool using a proxy model and a sample selection strategy and append it to the current batch.

Our work is related to [11] where the latent class centers are approximated utilizing an external pretrained model CLIP [12] and chooses a subset of sample which lies near the cluster centers. We do not use such a pretrained model. Rather we use our

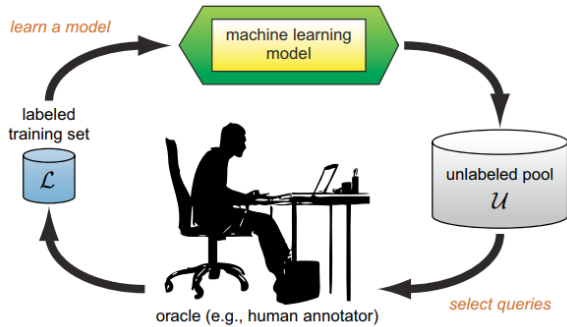


Fig. 1. Active learning loop [14]. An oracle annotates the most informative samples which is used to refine model predictions.

CL model features for informative sample selection. Researchers in [13] used a small proxy network to select samples in an active learning setup. But they consider active learning in the supervised domain (they require an oracle for every iteration of the active learning loop). Our work can be considered as an extension of their framework to the self supervised domain. Furthermore, this is the first work that considers data efficiency in CL for the domain of histopathology images (be specific how this helps to make it novel, does the algorithm change, can we include some domain related tricks, etc.). The contributions of our work are to

- increase CL efficiency in terms of time and sample complexity,
- provide a method to constrain the model into learning relevant representations by using active sampling, and
- improve CL efficiency in the histopathology domain.

II. METHOD

In this section, we describe the components in our proposed framework and formalize the methodology.

A. Contrastive Learning

SimCLR [5] proposed a simple framework for contrastive learning of visual representations by maximizing agreement between differently augmented views of the same sample via a contrastive loss in the latent space. Consider an unlabeled image pool U and x are the image samples $x \in U$.

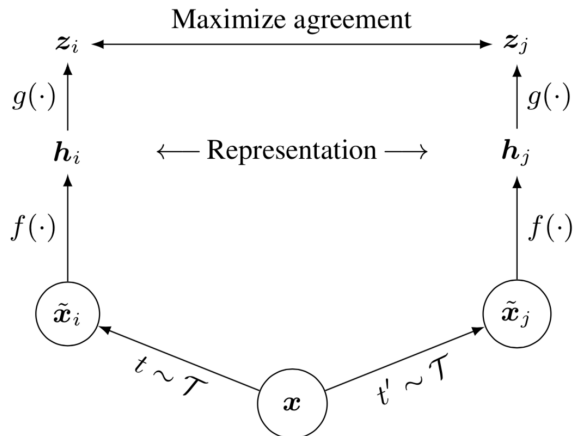


Fig. 2. SimCLR framework introduced in [5]. The model minimizes the distance (maximizes agreement) between feature representation of two augmented views \tilde{x}_i and \tilde{x}_j of the same image.

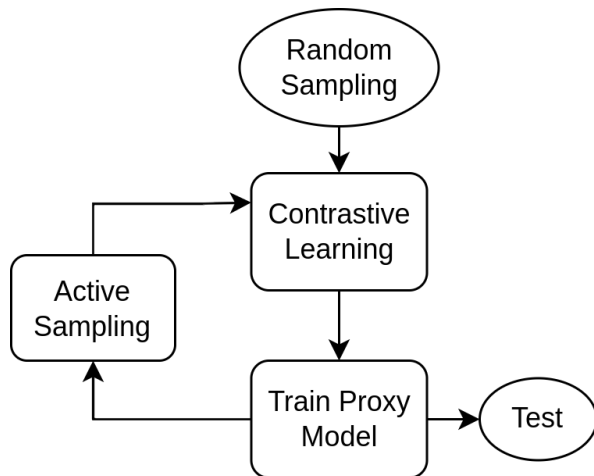


Fig. 3. The proposed framework speeds up the contrastive sampling process by actively selecting informative samples with the help of a small proxy network.

In CL, a minibatch of N samples are randomly sampled and each sample is applied with random data augmentation operations, resulting in N pairs of augmented samples or $2N$ augmented samples in total:

$$\tilde{x}_i = t(x), \tilde{x}_j = t'(x), t, t' \sim \mathcal{T}, \quad (1)$$

where two separate data augmentation operators, t and t' , are sampled from the same family of augmentations \mathcal{T} . Given one positive pair, other $2(N-1)$ data points are treated as negative samples.

The representation is produced by a base encoder $f(\cdot)$:

$$h_i = f(\tilde{x}_i), h_j = f(\tilde{x}_j). \quad (2)$$

The encoded representation is passed through a projection head $g(\cdot)$ which is a series of three fully connected layers. Experiments show that a projection head improves the quality of the encoded features h [5]:

$$z_i = g(h_i), z_j = g(h_j).$$

The CL loss $\mathcal{L}^{i,j}$ is defined using cosine similarity on the output of the projection head:

$$\mathcal{L}^{i,j} = -\log \frac{\exp[\text{sim}(z_i, z_j)/\tau]}{\sum_{k=1}^{2N} (1 - \delta_{ik}) \exp[\text{sim}(z_i, z_k)/\tau]},$$

where δ_{ik} is the Kronecker delta function which evaluates to 1 if $i = k$ and 0 otherwise. Note that, after training is completed, we throw away the projection head $g(\cdot)$ and use encoder $f(\cdot)$ and representation h to train a proxy model.

B. Proxy Model

The proxy model $f_p(\cdot)$ is a neural network with a single fully connected layer. We extract image features using the CL model encoder and train the proxy model on these features. The output of the proxy model is used to select informative samples from the unlabeled image pool.

C. Active Sampling

We extract the image features using the CL model and use active sampling strategies to select most informative samples. For this paper we use uncertainty sampling and coreset sampling.

1) *Uncertainty Sampling.*: Uncertainty sampling is the most common sampling criteria in which an active learner selects the instances about which it is least certain how to label. The uncertain samples normally reside near the class decision boundaries. We use entropy [15], the most common measure of uncertainty:

$$H(x_i) \equiv \sum_j P(y_j | x_i; \theta) \log P(y_j | x_i; \theta), \quad (3)$$

where y_j ranges over all possible labels and x_i is data. Entropy is an information-theoretic measure that quantifies information content.

2) *Coreset Sampling.*: Coreset formulates the active sampling problem as choosing a subset of samples that spans the dataset [16]. The subset selection problem is formulated as a k-center problem using a greedy approximation shown in Algorithm 1.

Algorithm 1 k-Center Greedy [16]

Input: data \mathbf{x}_i , existing unlabeled image pool \mathbf{s}^0 and a budget b
Initialize $\mathbf{s} = \mathbf{s}^0$
repeat
 $u = \arg \max_{i \in [n] \setminus \mathbf{s}} \min_{j \in \mathbf{s}} \Delta(\mathbf{x}_i, \mathbf{x}_j)$
 $\mathbf{s} = \mathbf{s} \cup \{u\}$
until $|\mathbf{s}| = b + |\mathbf{s}^0|$
return $\mathbf{s} \setminus \mathbf{s}^0$

Uncertainty sampling focuses on samples in the decision boundary, while coreset focuses on sample diversity. These are the two most common sampling methods used in the literature. A complete list of existing strategies can be found in [14].

D. Proposed Framework

The proposed framework is depicted in Fig. 3. Let U^t be the unlabeled image pool at iteration t , S_L is a small set of images with labels and S_{test} is the test set. We sample a initial random pool of images $S^t \subset U^t$ of budget b and update the unlabeled image pool, $U^t \leftarrow U^t \setminus S^t$. The subset S^t is used to train the SimCLR model. We freeze the encoder $f(\cdot)$ and extract features h_i , for $x_i \in S_L$. A proxy model f_p^t was trained using features h_i . This proxy model was used to find the next subset of images S^{t+1} to be included in the CL training set, $S^t \leftarrow S^t \cup S^{t+1}$. If uncertainty is used as sampling criterion, the entropy $H(x_i)$ is computed using outputs of $f_p^t(\cdot)$ and we select the top b samples with highest uncertainty. If coreset is used, we select b samples following the k-center greedy algorithm presented in Algorithm 1. This iterative process is continued for a given number of iterations T . Note that the weights of the SimCLR model are randomly initialized in the first iteration and training continues in the subsequent iterations using the learned weights in the previous iteration. The proxy network, however, is learned from random weights in each iteration. The set $S^t \cup S^{t+1}$

Algorithm 2 Contrastive Learning with Active Sampling

```

1: Input:  $S_L, U^t, g \circ f, f_p^t, T$ 
2: Output: trained encoder  $f(\cdot)$ 
3: Initialize:
    $S^0 \leftarrow$  Random sampling on  $U^0$ 
4:
5: for  $t = 0$  to  $T - 1$  do
6:   Train  $g \circ f$  using  $S^t$ 
7:   Train  $f_p^t$  using  $S_t$ 
8:    $U^t \leftarrow U^t \setminus S^t$ 
9:    $S^{t+1} \leftarrow$  Active Sampling on  $U^t$ 
10:   $S^t \leftarrow S^t \cup S^{t+1}$ 
11: end for

```

is used for the next iteration of CL training. This process continues for a set number of iterations T . The pseudocode for the algorithm of our proposed framework is presented in Algorithm 2.

III. EXPERIMENT AND RESULTS

A. Dataset

We used the Kather-19 dataset presented in [17]. The train set consists of 100,000 non-overlapping image patches from hematoxylin and eosin (H&E) stained histological images of human colorectal cancer (CRC) and normal tissue. Tissue classes are: adipose (ADI), background (BACK), debris (DEB), lymphocytes (LYM), mucus (MUC), smooth muscle (MUS), normal colon mucosa (NORM), cancer-associated stroma (STR), colorectal adenocarcinoma epithelium (TUM). These images were manually extracted from 86 H&E stained human cancer tissue slides from formalin-fixed paraffin-embedded (FFPE) samples from the NCT Biobank (National Center for Tumor Diseases, Heidelberg, Germany) and the UMM pathology archive (University Medical Center Mannheim, Mannheim, Germany). Tissue samples contained CRC primary tumor slides and tumor tissue from CRC liver metastases; normal tissue classes were augmented with non-tumorous regions from gastrectomy specimen to increase variability. The test set consists of 7180 image patches from 50 patients with colorectal adenocarcinoma (no overlap with patients in train set) collected from NCT tissue bank. Both the train and test set patches are 224×224 pixels

at 0.5 microns per pixel. All images are color-normalized using Macenko’s method [18]. We created an imbalanced dataset by setting the TUM tissues as the positive class and combining all the non-tumor (NON-TUM) as negative class. The train set had 14,317 TUM patches and 85,683 NON-TUM patches. While the the test set had 1233 TUM patches and 5947 NON-TUM patches.

B. Experimental Details

The SimCLR model was trained using 224×224 input images. To create two views of the same image the following augmentations were used: color jitter, random crop, random grayscale, Gaussian blur, horizontal and vertical flip, random rotation by ± 90 deg. The image intensities were divided by 255 and normalized by the ImageNet mean and standard deviation.

The training set is randomly split into two sets: an unlabeled pool U of 99,000 images and 1000 to train a proxy model (randomly sampled from the full train set). The original test set of size 7180 is used to evaluate the proxy model. The size of the subset sampled at each iteration for SSL is 1000, and the number of iterations, T , is 20. The CL model f_θ was a Resnet18 encoder [19] connected to a projection head that consisted of 3 fully connected layers with 128 units, the proxy model f_p was a linear layer with 512 units. Note that at each iteration, active sampling is done on a randomly selected subset of 10,000 to reduce computation and data redundancy. As the benchmark, we trained the SimCLR model for 100 epochs using the full unlabeled pool U and evaluated its feature quality by training the proxy model on the small labeled dataset. The proxy model was trained for 200 epochs, and its performance was evaluated at 20 epoch intervals on the test set. Then we trained the SimCLR model following our proposed framework using a subset of images. We considered uncertainty, coreset sampling as our active sampling methods. Also, random sampling of subsets was included as an ablation study to observe the absence of active sampling. At each iteration we trained the SimCLR model for 100 epochs and the proxy model for 40 epochs. The performance of the proxy model was evaluated at the end of each iteration. For both the experiments, the SimCLR

model was trained with a learning rate of 0.0001 and the proxy model with a learning rate of 0.001. The loss used for SimCLR was normalized cross-entropy with temperature 0.1, and for the classifier we used binary cross-entropy loss. For both models we used the Adam optimizer [20] with $\beta_1 = 0.9$, $\beta_2 = 0.999$. The training batch size is 128. Each experiment was run three times, and the average performance is reported.

C. Metrics

The evaluation metric used is the F1 score which accounts for the imbalance in the dataset. The F1 score is the harmonic average of precision (P) and recall (R).

$$F1 = \frac{2RP}{R + P}; R = \frac{TP}{TP + FN}, P = \frac{TP}{TP + FP} \quad (4)$$

Here, TP is true positive, FN is false negative, FP is false positive. F1 score is chosen due to the imbalance in the positive and negative classes in the images. We also computed the average run time for the benchmark and proposed method to reach a certain F1 score.

D. Results

For the benchmark experiment we observed a highest F1 of 0.84. To reach similar score the uncertainty and coreset based sampling strategy takes 7000 and 11,000 samples respectively (Fig. 4). Thus sample requirement is decreased by 93% and 89% respectively. Also, we observed that random sampling performs worse compared to the active sampling methods. The benchmark achieved its highest score at 100th epoch of SimCLR training and at the 150th epoch of the proxy model training. The average runtime for 100 epochs of SimCLR training is 538.70 min. To reach similar scores, the uncertainty based active sampling experiment required 7 iterations (7000 samples). The average time to train the SimCLR model for 7 iterations was 196.88 min. Average time to train proxy model and sample selection was 7.16 min. This resulted in a total average runtime of 204.4 min.

Similarly, k-center based sampling experiment required 11 iterations (11,000 samples). The average time to train the SimCLR model was 514.95

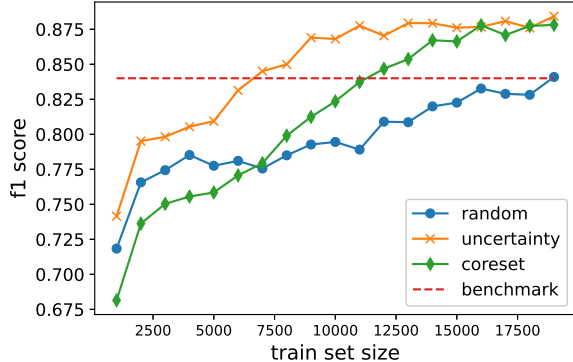


Fig. 4. Comparison of sampling strategies. The active sampling methods (uncertainty and coreset) requires less samples to reach the CL model trained on full set of images (benchmark).

min. Average time to train proxy model and sample selection was 23.70 min. This resulted in a total average runtime of 538.65 min. Due to uncertainty sampling there is a time reduction of 62% while coreset sampling requires similar amount of time. Further hyperparameter (such as SimCLR learning epochs, proxy model learning epochs, etc.) tuning might decrease these time requirements which is left for future research. The runtime comparisons are summarized in Table I.

TABLE I
RUNTIME COMPARISON

Method	Avg Runtime (min)	Time Reduction %
Benchmark	538.70	NA
Uncertainty	204.4	62
Coreset	538.65	0

IV. CONCLUSION

In this paper, we have demonstrated that active learning strategies can be used in CL to speed up training using less data. Also, using the uncertainty sampling we have proposed a feedback system for the contrastive learning framework to select the subset with the most amount of information related to the downstream task. We showed for histopathological cancer classification, we can achieve a speedup of 62% while using 93% less data. This method requires only a small labeled set. Future work could explore whether this number can

be reduced and how that would affect contrastive training. This research focused on classification as the downstream task. Future research can extend this to other tasks such as regression or segmentation.

REFERENCES

- [1] Carl Doersch, Abhinav Gupta, and Alexei A Efros. Unsupervised visual representation learning by context prediction. In *Proceedings of the IEEE international conference on computer vision*, pages 1422–1430, 2015.
- [2] Mehdi Noroozi and Paolo Favaro. Unsupervised learning of visual representations by solving jigsaw puzzles. In *Computer Vision—ECCV 2016: 14th European Conference, Amsterdam, The Netherlands, October 11–14, 2016, Proceedings, Part VI*, pages 69–84. Springer, 2016.
- [3] Richard Zhang, Phillip Isola, and Alexei A Efros. Colorful image colorization. In *Computer Vision—ECCV 2016: 14th European Conference, Amsterdam, The Netherlands, October 11–14, 2016, Proceedings, Part III 14*, pages 649–666. Springer, 2016.
- [4] Spyros Gidaris, Praveer Singh, and Nikos Komodakis. Unsupervised representation learning by predicting image rotations. *arXiv preprint arXiv:1803.07728*, 2018.
- [5] Ting Chen, Simon Kornblith, Mohammad Norouzi, and Geoffrey Hinton. A simple framework for contrastive learning of visual representations, 2020.
- [6] Ozan Ciga, Tony Xu, and Anne Louise Martel. Self supervised contrastive learning for digital histopathology. *Machine Learning with Applications*, 7:100198, 2022.
- [7] David Cohn, Les Atlas, and Richard Ladner. Improving generalization with active learning. *Machine learning*, 15(2):201–221, 1994.
- [8] Anders Krogh and Jesper Vedelsby. Neural network ensembles, cross validation, and active learning. In *Advances in neural information processing systems*, pages 231–238, 1995.
- [9] Yann LeCun, Yoshua Bengio, and Geoffrey Hinton. Deep learning. *nature*, 521(7553):436–444, 2015.
- [10] Samuel Budd, Emma C Robinson, and Bernhard Kainz. A survey on active learning and human-in-the-loop deep learning for medical image analysis. *arXiv preprint arXiv:1910.02923*, 2019.
- [11] Siddharth Joshi and Baharan Mirzasoleiman. Data-efficient contrastive self-supervised learning: Easy examples contribute the most. *arXiv preprint arXiv:2302.09195*, 2023.
- [12] Alec Radford, Jong Wook Kim, Chris Hallacy, Aditya Ramesh, Gabriel Goh, Sandhini Agarwal, Girish Sastry, Amanda Askell, Pamela Mishkin, Jack Clark, et al. Learning transferable visual models from natural language supervision. In *International conference on machine learning*, pages 8748–8763. PMLR, 2021.
- [13] Cody Coleman, Christopher Yeh, Stephen Mussmann, Baharan Mirzasoleiman, Peter Bailis, Percy Liang, Jure Leskovec, and Matei Zaharia. Selection via proxy: Efficient data selection for deep learning. *arXiv preprint arXiv:1906.11829*, 2019.
- [14] Burr Settles. Active learning literature survey. 2009.
- [15] Claude E Shannon. A mathematical theory of communication. *The Bell system technical journal*, 27(3):379–423, 1948.
- [16] Ozan Sener and Silvio Savarese. Active learning for convolutional neural networks: A core-set approach. *arXiv preprint arXiv:1708.00489*, 2017.
- [17] Jakob Nikolas Kather, Niels Halama, and Alexander Marx. 100,000 histological images of human colorectal cancer and healthy tissue, April 2018.
- [18] Marc Macenko, Marc Niethammer, J. S. Marron, David Borland, John T. Woosley, Xiaojun Guan, Charles Schmitt, and Nancy E. Thomas. A method for normalizing histology slides for quantitative analysis. In *2009 IEEE International Symposium on Biomedical Imaging: From Nano to Macro*, pages 1107–1110, 2009.
- [19] Kaiming He, Xiangyu Zhang, Shaoqing Ren, and Jian Sun. Deep residual learning for image recognition. In *Proceedings of the IEEE conference on computer vision and pattern recognition*, pages 770–778, 2016.
- [20] Diederik P Kingma and Jimmy Ba. Adam: A method for stochastic optimization. *arXiv preprint arXiv:1412.6980*, 2014.